

# Magnetic structure of heavy fermion $\text{Ce}_2\text{RhIn}_8$

Wei Bao, P.G. Pagliuso, J.L. Sarrao, J.D. Thompson and Z. Fisk\*  
*Los Alamos National Laboratory, Los Alamos, NM 87545*

J. W. Lynn

*NIST Center for Neutron Research, National Institute of Standards and Technology, Gaithersburg, MD 20899*  
 (June 16, 2024)

The magnetic structure of the heavy fermion antiferromagnet  $\text{Ce}_2\text{RhIn}_8$  is determined using neutron diffraction. It is a collinear antiferromagnet with a staggered moment of  $0.39(4)\mu_B$  per Ce at 1.6 K, tilted  $38^\circ$  from the tetragonal  $c$  axis. In spite of its layered crystal structure, the phases for the magnetic moments are the same as those in the cubic parent antiferromagnet  $\text{CeIn}_3$ . This suggests that the cubic  $\text{CeIn}_3$  building blocks have a stronger influence on magnetic correlations than intervening layers, which gives the material its apparent two-dimensional lattice structure and renders  $\text{CeRhIn}_5$  an incommensurate antiferromagnet.

Superconducting heavy fermion materials belong to a special class of correlated electron systems where unconventional superconductivity may be mediated by magnetic fluctuations [1]. Until recently, there were only five U-based heavy fermion materials showing superconductivity at ambient pressure [2] in addition to the original heavy fermion superconductor  $\text{CeCu}_2\text{Si}_2$  [3]. Three Ce-based heavy fermion materials isostructural to  $\text{CeCu}_2\text{Si}_2$  and cubic  $\text{CeIn}_3$  become superconductors under pressure. Recently, superconductivity has been discovered in a new structure class of heavy fermion materials with chemical formulas  $\text{Ce}M\text{In}_5$ . While the  $M=\text{Rh}$  member superconducts below 2.1 K under 17kbar [4], the  $M=\text{Ir}$  and  $\text{Co}$  members superconduct below 0.4 K and 2.3 K, respectively, at ambient pressure [5,6]. The high superconducting transition temperatures of the new materials hold the record for heavy fermion superconductors. Thermodynamic and transport measurements at low temperature are consistent with unconventional superconductivity in which there are lines of nodes in the superconducting gap [7].

Because  $\text{CeIn}_3$  and  $\text{Ce}M\text{In}_5$  belong to the  $\text{Ce}_nM_m\text{In}_{3n+2m}$  family of structures, they present a unique opportunity for investigating the influence of systematic structure modifications on the superconducting and magnetic properties [8]. In particular, it is interesting to compare  $\text{CeIn}_3$  and  $\text{CeRhIn}_5$ , which are the  $n=\infty$  and  $n=1$  members of the  $\text{Ce}_n\text{RhIn}_{3n+2}$  subfamily, and can be viewed as periodic stacking of  $n$ -layers of  $\text{CeIn}_3$  on a layer of  $M\text{In}_2$  [9,10]. Both are antiferromagnetic at ambient pressure with  $T_N = 10$  K for  $\text{CeIn}_3$  [11] and  $T_N = 3.8$  K for  $\text{CeRhIn}_5$  [4,12]. Both become superconductors when subjected to pressure [4,13], with the superconducting transition temperature of  $\text{CeRhIn}_5$  being one order of magnitude higher than that for  $\text{CeIn}_3$ . This raises a fundamental question about the role of the intervening  $M\text{In}_2$  layers on both the superconductivity and antiferromagnetism. Our study of  $\text{Ce}_2\text{RhIn}_8$ , which is the  $n=2$  member of this heavy fermion sub-family, is intended to shed light on this question by changing the

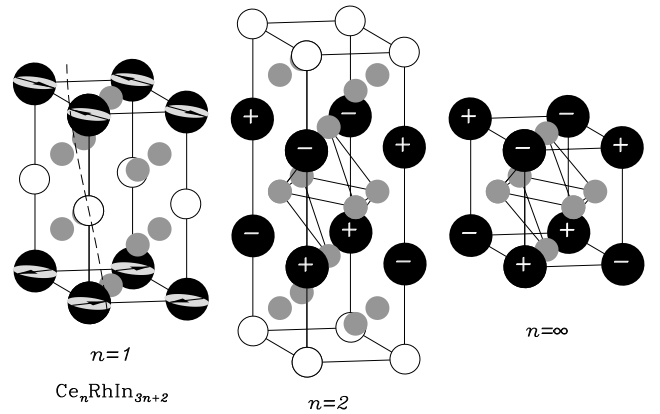


FIG. 1. The magnetic structure of  $\text{Ce}_2\text{RhIn}_8$  ( $n=2$ ) in a structural unit cell is shown together with  $\text{CeRhIn}_5$  ( $n=1$ ) [16] and  $\text{CeIn}_3$  ( $n=\infty$ ) [14,15]. The magnetic moment is  $0.39\mu_B$  per Ce in  $\text{Ce}_2\text{RhIn}_8$  and it points  $38^\circ$  from the  $c$  axis. The solid circle denotes Ce, the shaded circle In, and the open circle Rh. The disk for  $\text{CeRhIn}_5$  denotes the plane in which the ordered moment rotates.

ratio of the  $\text{CeIn}_3$  and  $\text{RhIn}_2$  layers.

Antiferromagnetic structures for both  $\text{CeIn}_3$  and  $\text{CeRhIn}_5$  have been determined previously. Cubic  $\text{CeIn}_3$  has a simple commensurate magnetic order with wave vector  $(1/2, 1/2, 1/2)$  below its Néel temperature. The staggered magnetic moment is  $0.48\text{--}0.65\mu_B$  per Ce [14,15]. In contrast, magnetic moments of Ce ions in tetragonal  $\text{CeRhIn}_5$  form an incommensurate transverse spiral below  $T_N = 3.8$  K, with wave vector  $(1/2, 1/2, 0.297)$  [16] (refer to Fig. 1). The staggered moment of  $0.26\mu_B$  per Ce at 1.4 K is smaller than that for  $\text{CeIn}_3$ . In this paper, we report the magnetic structure for  $\text{Ce}_2\text{RhIn}_8$ , which orders at  $T_N = 2.8$  K [8]. The commensurate antiferromagnetic structure for this  $n=2$  material closely resembles that for  $\text{CeIn}_3$  ( $n=\infty$ ), rather than the magnetic spiral of  $\text{CeRhIn}_5$  ( $n=1$ ). This sug-

TABLE I. Magnetic Bragg intensity,  $\sigma_{obs}$ , defined in Eq. (1), observed at 1.6 K in units of  $10^{-3}$  barns per  $\text{Ce}_2\text{RhIn}_8$ . The theoretical intensity,  $\sigma_{cal}$ , is calculated using Eq. (2) and (3) with  $\beta = 52^\circ$  and  $M = 0.39\mu_B/\text{Ce}$ .

$\mathbf{q}$	$\sigma_{obs}$	$\sigma_{cal}$
(0.5 0.5 -1)	52(1)	46.2
(0.5 0.5 0)	0.0(3)	0.0
(0.5 0.5 1)	49(1)	46.2
(0.5 0.5 2)	19(1)	18.9
(0.5 0.5 3)	6.4(4)	5.5
(0.5 0.5 4)	21(1)	23.2
(0.5 0.5 6)	7.5(7)	7.6
(1.5 1.5 0)	0.0(8)	0.0
(1.5 1.5 1)	18(1)	24.8

gests a strong influence of the cubic  $\text{CeIn}_3$  structural unit on magnetic correlations in this family of heavy fermion materials.

Single crystals of  $\text{Ce}_2\text{RhIn}_8$  were grown from an In flux. They crystallize in the tetragonal  $\text{Ho}_2\text{CoGa}_8$  structure (space group #123,  $P4/\text{mmm}$ ) [9], with lattice parameters  $a = 4.665\text{\AA}$  and  $c = 12.244\text{\AA}$  at room temperature. The sample used in this study was a well-faceted rectangular plate of dimension  $\sim 4 \times 4 \times 0.7$  mm and weight of 88 mg. The largest surface is the (001) plane. Neutron diffraction experiments were performed at NIST using the thermal triple-axis spectrometer BT2 in a two-axis mode. The horizontal collimations were 60-40-40-open. Neutrons with incident energy  $E = 35$  meV were selected using the (002) reflection of a pyrolytic graphite (PG) monochromator. The neutron penetration length at this energy is 1.8 mm, which is substantially longer than the thickness of the sample. No rocking-angle dependent absorption was noticed. PG filters of total 9 cm thickness were used to remove higher order neutrons. The sample temperature was regulated by a top loading pumped He cryostat.

Temperature-dependent magnetic Bragg peaks were found at  $(m/2, n/2, l)$  with  $m$  and  $n$  odd integers and  $l$  non-zero integers. This corresponds to a magnetic unit cell that doubles the structural unit cell in the basal plane and contains four magnetic Ce ions. Rocking scans at  $(1/2, 1/2, 0)$  and  $(1/2, 1/2, \bar{1})$ , taken at 1.6 K, are shown in Fig. 2(a). The intensity of the  $(1/2, 1/2, 1)$  peak is shown in Fig. 2(b) as the square of the order parameter of the magnetic phase transition. Integrated intensities of magnetic Bragg peaks from such rocking scans are normalized to structural Bragg peaks (001), (002), (003), (005), (006) and (220) to yield magnetic scattering cross sections,  $\sigma(\mathbf{q}) = I(\mathbf{q}) \sin(\theta_4)$ , in absolute units (see Table I). In such units, the magnetic cross section is [17]

$$\sigma(\mathbf{q}) = \left(\frac{\gamma r_0}{2}\right)^2 \langle M \rangle^2 |f(q)|^2 \sum_{\mu, \nu} (\delta_{\mu\nu} - \hat{q}_\mu \hat{q}_\nu) \mathcal{F}_\mu^*(\mathbf{q}) \mathcal{F}_\nu(\mathbf{q}), \quad (1)$$

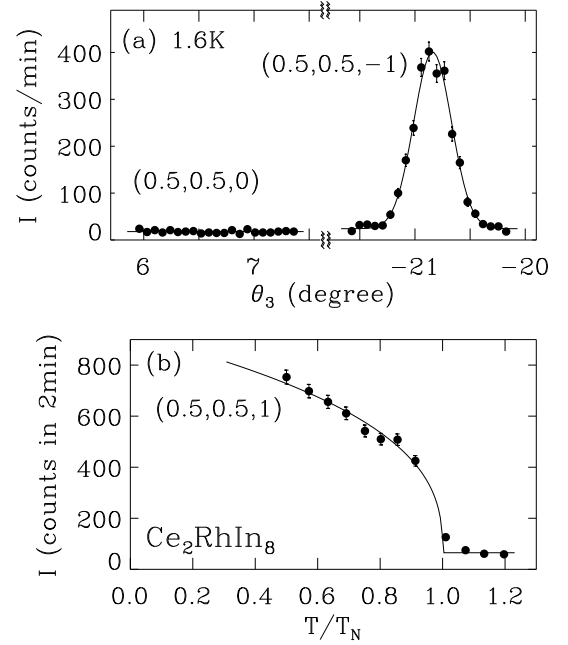


FIG. 2. (a) Elastic rocking scans through magnetic Bragg points  $(1/2, 1/2, 0)$  and  $(1/2, 1/2, -1)$  at 1.6 K. The  $(1/2, 1/2, 0)$  is forbidden for this magnetic structure. (b) Intensity of  $(1/2, 1/2, 1)$  as a function of  $T/T_N$ . The Néel temperature is 2.8 K.

where  $(\gamma r_0/2)^2 = 0.07265$  barns/ $\mu_B^2$ ,  $M$  is the staggered moment of the Ce ion,  $f(q)$  the  $\text{Ce}^{3+}$  magnetic form factor [18],  $\hat{\mathbf{q}}$  the unit vector of  $\mathbf{q}$ , and  $\mathcal{F}_\mu(\mathbf{q})$  the  $\mu$ th Cartesian component of magnetic structure factor per  $\text{Ce}_2\text{RhIn}_8$ .

Forbidden peaks at  $(m/2, m/2, 0)$  provide an important clue to the magnetic structure of  $\text{Ce}_2\text{RhIn}_8$ . They could be due to magnetic moments aligning along the  $[110]$  direction. However, magnetic twinning in this tetragonal material will yield finite intensities at these reciprocal points. Another, more reasonable, cause is that the nearest-neighbor magnetic moments along the  $c$  axis are antiparallel. The phase between the next nearest-neighbor magnetic moments along the  $c$  axis and the phases of magnetic moments in a basal layer are already determined by the magnetic wave vector. This yields a collinear antiferromagnetic structure (refer to Fig. 1) with magnetic cross sections per  $\text{Ce}_2\text{RhIn}_8$

$$\sigma(\mathbf{q}) = 8 \left(\frac{\gamma r_0}{2}\right)^2 \langle M \rangle^2 |f(q)|^2 \langle 1 - (\hat{\mathbf{q}} \cdot \hat{\mathbf{s}})^2 \rangle \sin^2(l\epsilon), \quad (2)$$

where  $2\epsilon = 0.38c$  is the separation between the nearest-neighbor Ce ions along the  $c$  axis,  $\hat{\mathbf{s}}$  is the unit vector of the magnetic moment, and the average,  $\langle 1 - (\hat{\mathbf{q}} \cdot \hat{\mathbf{s}})^2 \rangle$ , is over magnetic domains.

Fig. 3 shows  $\sigma_{obs}(\mathbf{q})/|f(q)|^2 \sim \langle 1 - (\hat{\mathbf{q}} \cdot \hat{\mathbf{s}})^2 \rangle \sin^2(l\epsilon)$

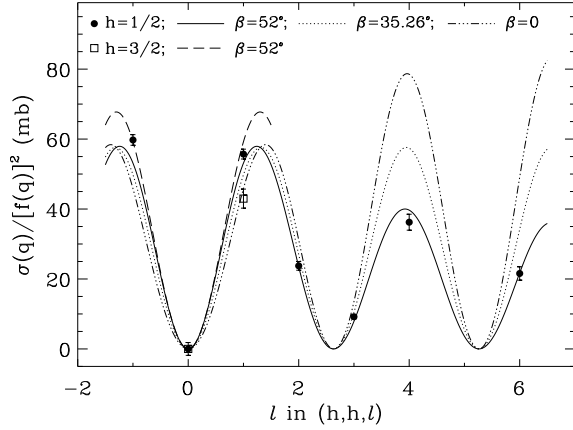


FIG. 3. The  $l$  dependence of the magnetic cross-section,  $\sigma$ , divided by the form factor  $|f(q)|^2$ . The theoretical curves are calculated using Eq. (2) and (3) with  $M = 0.39\mu_B$  and various values specified in the figure for the moment tilt angle,  $\beta$ .

as a function of the  $l$  index of  $\mathbf{q}$ . The structure factor,  $8\sin^2(l\epsilon)$ , not only accounts for the forbidden  $l = 0$  magnetic peaks, but it also accounts for the strong oscillation of  $\sigma_{obs}$  as a function of  $l$ . The remaining, smooth  $l$  dependence is to be accounted for by the polarization factor  $\langle 1 - (\hat{\mathbf{q}} \cdot \hat{\mathbf{s}})^2 \rangle$ .

Denote the angle between  $\mathbf{q}$  and the basal plane as  $\alpha$ , and the angle between the basal plane and the magnetic moment as  $\beta$ . Assuming equal occupations among magnetic twins, we have

$$\langle 1 - (\hat{\mathbf{q}} \cdot \hat{\mathbf{s}})^2 \rangle = 1 - \frac{\cos^2 \alpha \cos^2 \beta + 2 \sin^2 \alpha \sin^2 \beta}{2}. \quad (3)$$

For a magnetic moment lying in the basal plane,  $\beta = 0$ , which is the case for  $\text{CeRhIn}_5$  [16,12], the polarization factor varies too much. The resulting theoretical curve does not fit the data (refer to the dot-dashed line in Fig. 3). For  $\beta = 35.26^\circ$ , which corresponds to  $\mathbf{s}$  in the  $\langle 111 \rangle$  directions in a cubic system, the polarization factor averages to a constant,  $2/3$ . The resulting theoretical curve is a better fit (refer to the dotted line in Fig. 3) than that for  $\beta = 0$ , but it is still not satisfactory. The best least-squares fit (refer to the solid and dashed lines for  $h = k = 1/2$  and  $h = k = 3/2$  respectively) yields  $\beta = 52(2)^\circ$ . The staggered magnetic moment is determined at 1.6 K to be  $M = 0.39(4)\mu_B$  per Ce.

Having determined the magnetic structure of  $\text{Ce}_2\text{RhIn}_8$ , now we consider the systematics relating the magnetic structure and lattice structure in  $\text{Ce}_n\text{RhIn}_{3n+2}$  (see Fig. 1). In the  $a$ - $b$  plane, the magnetic moments of the Ce ions form a square lattice, surrounded by In ions, in all three materials. They all are simple, nearest-neighbor antiferromagnets in the basal plane. In  $\text{CeRhIn}_5$ , this Ce antiferromagnetic plane alternates with the  $\text{RhIn}_2$  layer. Magnetic correlations across the  $\text{RhIn}_2$  layer are incommensurate, with neighboring magnetic moments being rotated

by  $107^\circ$  [16]. The local structure environment in the vertical  $a$ - $c$  or the  $b$ - $c$  plane within the  $\text{CeIn}_3$  double layer in  $\text{Ce}_2\text{RhIn}_8$  is very similar to that in the basal layer. The same nearest-neighbor antiferromagnetic correlations exist in the double layers. It is interesting that now across the  $\text{RhIn}_2$  layer the Ce moments are antiparallel instead of rotated by  $107^\circ$ . The insertion of the  $\text{RhIn}_2$  layers between  $\text{CeIn}_3$  bilayers, thus, does not modify the magnetic order relative to cubic  $\text{CeIn}_3$ . This suggests  $\text{CeRhIn}_5$  as a unique member of the  $\text{Ce}_n\text{RhIn}_{3n+2}$  family, and the  $n \geq 2$  members are likely to be magnetically similar to cubic  $\text{CeIn}_3$ . Searching for heavy fermion materials with two-dimensional magnetism seems more profitable if one could find a  $\text{Ce}M_m\text{In}_{3+2m}$  structure family, where  $m$   $\text{MIn}_2$  layers separate a single  $\text{CeIn}_3$  layer.

Another interesting difference between the  $n = 1$  and the  $n = 2$  materials concerns the magnetic moment orientation. In  $\text{CeRhIn}_5$ , the moments rotate in the  $a$ - $b$  plane, indicating a  $XY$  type magnetic anisotropy. In  $\text{Ce}_2\text{RhIn}_8$ , the magnetic moments point  $52^\circ$  from the basal plane. Different local anisotropic fields, together with isotropic exchange and crystal fields, likely contribute to the different magnetic structures in the two materials [19]. We also notice that the staggered moment is a monotonic function of  $n$  for the three members of the structure series, in contrast to the behavior of  $T_N$ . The  $T_N/\langle M \rangle^2$  is largest for  $\text{CeRhIn}_5$  and smallest for  $\text{Ce}_2\text{RhIn}_8$  in the group. A similar trend in  $T_N$  has been found in  $\text{Nd}_n\text{RhIn}_{3n+2}$  and has been attributed to crystal field effects [20]. A detailed understanding of the magnetic interaction in these materials is necessary in pursuing the origin of unconventional superconductivity in these heavy fermion metals.

In conclusion, we find the magnetic structure of  $\text{Ce}_2\text{RhIn}_8$  to be closely related to that of cubic  $\text{CeIn}_3$ . The staggered moment is  $0.39(4)\mu_B$  per Ce at 1.6 K and it points  $52^\circ$  from the  $a$ - $b$  plane. Understanding the different magnetic structures in  $\text{Ce}_2\text{RhIn}_8$  and  $\text{CeRhIn}_5$  may help us understand the enormous enhancement in the superconducting transition temperature of  $\text{CeRhIn}_5$  over its cubic relative.

We thank M. E. Zhitomirsky and M. F. Hundley for useful discussions. WB thanks D. C. Dender for technical assistance at NIST. Work at Los Alamos was performed under the auspices of the US Department of Energy. ZF gratefully acknowledges NSF support at FSU. PGP acknowledges FAPESP for partial support.

- 
- [1] H. R. Ott and Z. Fisk, in *Handbook on the Physics and Chemistry of Actinides*, eds., A. J. Freeman and G. H. Lander, North-Holland, Amsterdam (1987).
  - [2] R. H. Heffner and M. R. Norman, *Comments Cond. mat. Phys.* **17**, 361 (1996).
  - [3] F. Steglich, J. Aarts, C. D. Bredl, W. Lieka, D. Meschede,

- W. Fraz, and H. Schääfer, Phys. Rev. Lett. **43**, 1982 (1979).
- [4] H. Hegger, C. Petrovic, E.G. Moshopoulou, M.F. Hundley, J.L. Sarrao, Z. Fisk, and J.D. Thompson, Phys. Rev. Lett. **84**, 4986 (2000).
  - [5] C. Petrovic, R. Movshovich, M. Jaime, P. G. Pagliuso, M.F. Hundley, J.L. Sarrao, Z. Fisk, and J.D. Thompson, Europhys. Lett. **53**, 354 (2001).
  - [6] C. Petrovic, P. G. Pagliuso, M.F. Hundley, R. Movshovich, J.L. Sarrao, J.D. Thompson, Z. Fisk and P. Monthoux, unpublished (2001).
  - [7] R. Movshovich, M. Jaime, J.D. Thompson, C. Petrovic, Z. Fisk, P. G. Pagliuso, and J.L. Sarrao, cond-mat/0011365 (2001).
  - [8] J.D. Thompson, et al., cond-mat/0012260, to appear in JMMM (2001).
  - [9] Yu. N. Grin, et al., Sov. Phys. Crystallogr. **24**, 137 (1979).
  - [10] E.G. Moshopoulou, Z. Fisk, J. L. Sarrao and J. D. Thompson, submitted to J. Solid State Chem. (2000).
  - [11] K. H. J. Buschow, H. W. de Wijn and A. M. van Diepen, J. Chem. Phys. **50**, 137 (1969).
  - [12] N.J. Curro, P.C. Hammel, P.G. Pagliuso, J.L. Sarrao, J.D. Thompson, and Z. Fisk, Phys. Rev. B **62**, R6100 (2000).
  - [13] N.D. Mathur, F.M. Grosche, S.R. Julian, I.R. Walker, D.M. Freye, R.K.W. Haselwimmer, and G.G. Lonzarich, Nature **394**, 39 (1998).
  - [14] A. Benoit, J.X. Boucherle, P. Convert, J. Flouquet, J. Palteau, and J. Schweizer, Solid State Commun. **34**, 293 (1980).
  - [15] J.M. Lawrence and S.M. Shapiro, Phys. Rev. B **22**, 4379 (1980).
  - [16] W. Bao, P. G. Pagliuso, J. L. Sarrao, J. D. Thompson, Z. Fisk, J. W. Lynn, and R. W. Erwin, Phys. Rev. B **62**, R14621 (2000).
  - [17] G. L. Squires, *Introduction to the Theory of Thermal Neutron Scattering* (Cambridge University Press, Cambridge, 1978).
  - [18] M. Blume, A. J. Freeman and R. E. Watson, J. Chem. Phys. **37**, 1245 (1962).
  - [19] J. Jensen and A. R. Mackintosh, *Rare Earth Magnetism: Structures and Excitations* (Clarendon Press, Oxford, 1991).
  - [20] P. G. Pagliuso, J.D. Thompson, M.F. Hundley, J.L. Sarrao, Phys. Rev. B **62**, 12266 (2000).